Stem Cell Reports, Volume *12*

Supplemental Information

X-Chromosome Dosage Modulates Multiple Molecular and Cellular Properties of Mouse Pluripotent Stem Cells Independently of Global DNA Methylation Levels

Juan Song, Adrian Janiszewski, Natalie De Geest, Lotte Vanheer, Irene Talon, Mouna El Bakkali, Taeho Oh, and Vincent Pasque

Figure S1

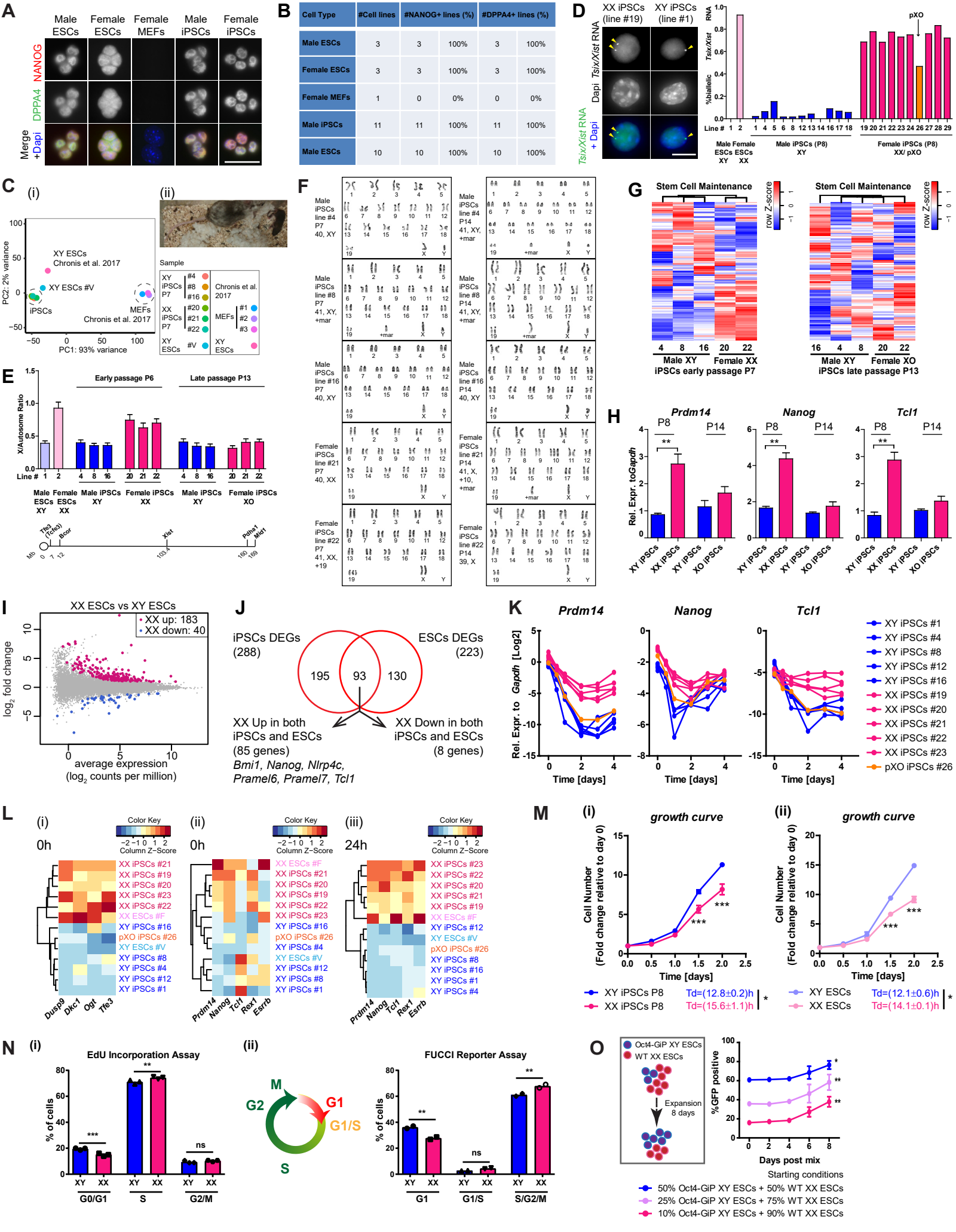
A
Male ESCs
Female ESCs
Female MEFs
Male iPSCs
Female iPSCs
NANOG
DPPA4
Merge +Dapi
B
Cell Type | #Cell lines | #NANOG+ lines (%) | #DPPA4+ lines (%)
Male ESCs | 3 | 3 | 100% | 3 | 100%
Female ESCs | 3 | 3 | 100% | 3 | 100%
Female MEFs | 1 | 0 | 0% | 0 | 0%
Male iPSCs | 11 | 11 | 100% | 11 | 100%
Male ESCs | 10 | 10 | 100% | 10 | 100%
D
XX iPSCs (line #19)
XY iPSCs (line #1)
Tsix/Xist RNA
Dapi
Tsix/Xist RNA + Dapi
RNA Tsix/Xist
%biallelic
pXO
Line # 1 2 1 4 5 6 8 12 13 14 16 17 18 19 20 21 22 23 24 26 27 28 29
Male ESCs XY
Female ESCs XX
Male iPSCs (P8) XY
Female iPSCs (P8) XX/ pXO
C
(i)
(ii)
PC2: 2% variance
PC1: 93% variance
XY ESCs Chronis et al. 2017
XY ESCs #V
iPSCs
MEFs Chronis et al. 2017
Sample
XY iPSCs P7 #4 #8 #16
XX iPSCs P7 #20 #21 #22
XY ESCs #V
Chronis et al. 2017
MEFs #1 #2 #3
XY ESCs
F
Male iPSCs line #4 P7 40, XY
Male iPSCs line #8 P7 41, XY, +mar
Male iPSCs line #16 P7 40, XY
Female iPSCs line #21 P7 40, XX
Female iPSCs line #22 P7 41, XX, +19
Male iPSCs line #4 P14 41, XY, +mar
Male iPSCs line #8 P14 41, XY, +mar
Male iPSCs line #16 P14 40, XY
Female iPSCs line #21 P14 41, X, +10, +mar
Female iPSCs line #22 P14 39, X
G
Stem Cell Maintenance
row Z-score
Male XY iPSCs early passage P7
Female XX
Stem Cell Maintenance
row Z-score
Male XY iPSCs late passage P13
Female XO
E
X/Autosome Ratio
Early passage P6
Late passage P13
Line # 1 2 4 8 16 20 21 22 4 8 16 20 21 22
Male ESCs XY
Female ESCs XX
Male iPSCs XY
Female iPSCs XX
Male iPSCs XY
Female iPSCs XO
Tfe3 (Tcfe3)
Bcor
Xist
Pdha1
Mid1
H
Prdm14
Nanog
Tcl1
P8
P14
Rel. Expr. to Gapdh
XY iPSCs
XX iPSCs
XY iPSCs
XO iPSCs
I
XX ESCs vs XY ESCs
XX up: 183
XX down: 40
log2 fold change
average expression
(log2 counts per million)
J
iPSCs DEGs (288)
ESCs DEGs (223)
195
93
130
XX Up in both iPSCs and ESCs (85 genes)
Bmi1, Nanog, Nlrp4c, Pramel6, Pramel7, Tcl1
XX Down in both iPSCs and ESCs (8 genes)
K
Prdm14
Nanog
Tcl1
Rel. Expr. to Gapdh [Log2]
Time [days]
XY iPSCs #1
XY iPSCs #4
XY iPSCs #8
XY iPSCs #12
XY iPSCs #16
XX iPSCs #19
XX iPSCs #20
XX iPSCs #21
XX iPSCs #22
XX iPSCs #23
pXO iPSCs #26
L
(i) 0h
(ii) 0h
(iii) 24h
Color Key
Column Z-Score
XX iPSCs #21
XX iPSCs #19
XX iPSCs #20
XX iPSCs #23
XX iPSCs #22
XX ESCs #F
XY iPSCs #16
pXO iPSCs #26
XY ESCs #V
XY iPSCs #8
XY iPSCs #4
XY iPSCs #12
XY iPSCs #1
Dusp9
Dkc1
Ogt
Tfe3
XX ESCs #F
XX iPSCs #21
XX iPSCs #20
XX iPSCs #19
XX iPSCs #22
XX iPSCs #23
XY iPSCs #16
pXO iPSCs #26
XY ESCs #V
XY iPSCs #4
XY iPSCs #12
XY iPSCs #8
XY iPSCs #1
Prdm14
Nanog
Tcl1
Rex1
Esrrb
XX iPSCs #23
XX iPSCs #22
XX iPSCs #20
XX iPSCs #21
XX iPSCs #19
XX ESCs #F
XY iPSCs #12
XY ESCs #V
pXO iPSCs #26
XY iPSCs #8
XY iPSCs #16
XY iPSCs #1
XY iPSCs #4
M
(i) growth curve
(ii) growth curve
Cell Number (Fold change relative to day 0)
Time [days]
XY iPSCs P8 Td=(12.8±0.2)h
XX iPSCs P8 Td=(15.6±1.1)h
XY ESCs Td=(12.1±0.6)h
XX ESCs Td=(14.1±0.1)h
N
(i) EdU Incorporation Assay
% of cells
G0/G1
S
G2/M
(ii) FUCCI Reporter Assay
G1
G1/S
S/G2/M
M
G2
G1
G1/S
S
O
Oct4-GiP XY ESCs
WT XX ESCs
Expansion 8 days
%GFP positive
Days post mix
Starting conditions
50% Oct4-GiP XY ESCs + 50% WT XX ESCs
25% Oct4-GiP XY ESCs + 75% WT XX ESCs
10% Oct4-GiP XY ESCs + 90% WT XX ESCs

Figure S2

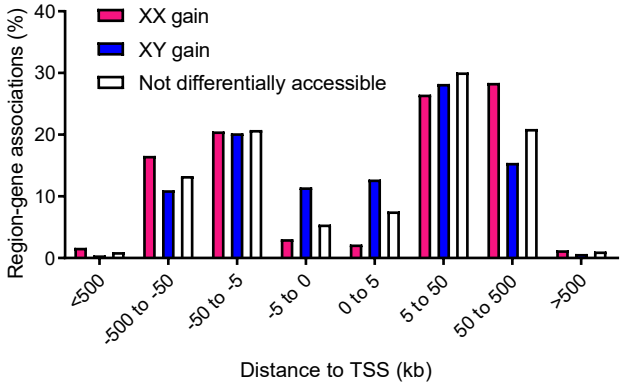

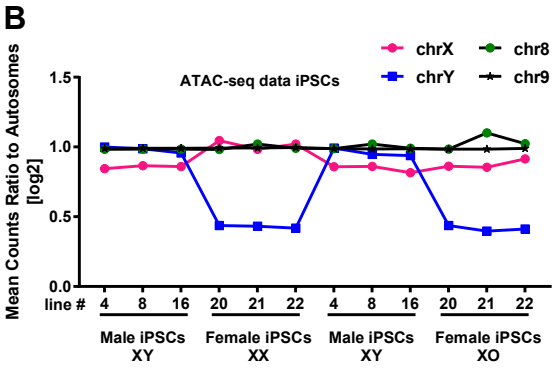

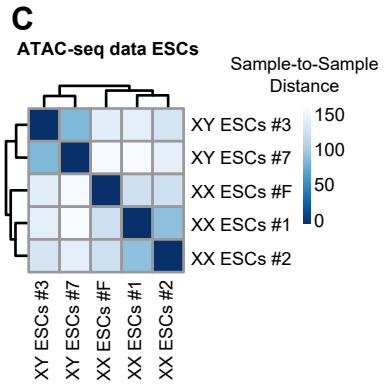

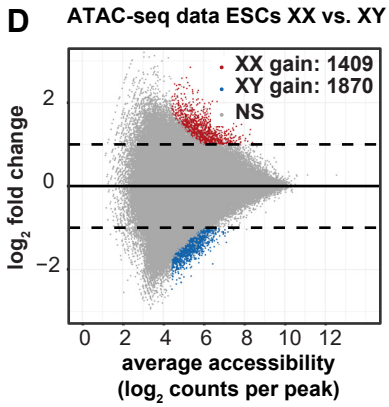

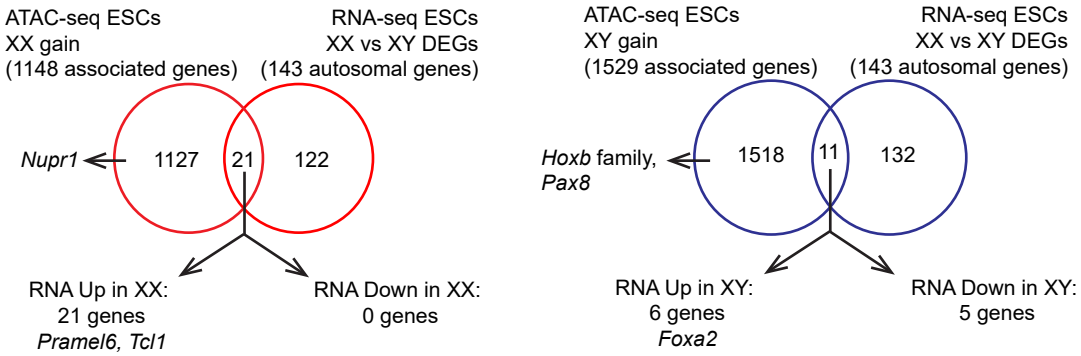

F

ESCs XX gain: 1409 peaks

#	Motif	Name	p-value	% of targets with Motif
1		KLF5	1e-98	57.27%
2		KLF6	1e-68	44.78%
3		Sox2	1e-49	36.27%
4		Klf4	1e-44	22.43%
5		Sox3	1e-43	55.57%
6		Sox15	1e-43	39.89%
7		EKLF	1e-41	16.32%
8		Sox17	1e-41	30.16%
9		KLF3	1e-40	23.85%
10		Sox6	1e-39	50.75%
11		Rfx2	1e-39	8.73%
12		Sox10	1e-38	53.02%
13		RFX	1e-38	8.09%
14		KLF14	1e-36	56.35%
15		X-box	1e-32	9.01%
26		Zic3	1e-16	22.00%

G

ESCs XY gain: 1870 peaks

#	Motif	Name	p-value	% of targets with Motif
1		Fra1	1e-789	74.12%
2		Atf3	1e-783	78.29%
3		JunB	1e-763	72.83%
4		BATF	1e-746	16.03%
5		AP-1	1e-719	78.82%
6		Fosl2	1e-668	56.95%
7		Jun-AP1	1e-556	46.26%
8		Bach2	1e-246	27.86%
9		NF-E2	1e-57	7.70%
10		Pitx1:Ebox	1e-52	13.58%
11		RUNX-AML	1e-50	32.03%
12		Bach1	1e-49	6.90%
13		MafK	1e-48	16.10%
14		RUNX2	1e-47	37.86%

J

iPSCs XX and XY common regions: 282740 peaks

#	Motif	Name	p-value	% of targets with Motif
1		CTCF	1e-6495	11.02%
2		Fosl2	1e-5114	14.80%
3		BORIS	1e-5021	12.76%
4		Jun-AP1	1e-5012	11.80%
5		Fra1	1e-5010	20.54%
6		JunB	1e-4762	20.36%
7		Atf3	1e-4737	23.21%
8		AP-1	1e-4239	25.01%
9		BATF	1e-4191	22.86%
10		Bach2	1e-2741	8.79%
11		KLF5	1e-2351	39.80%
12		KLF3	1e-2119	18.46%
13		KLF6	1e-1866	32.00%
14		Sp5	1e-1835	30.36%

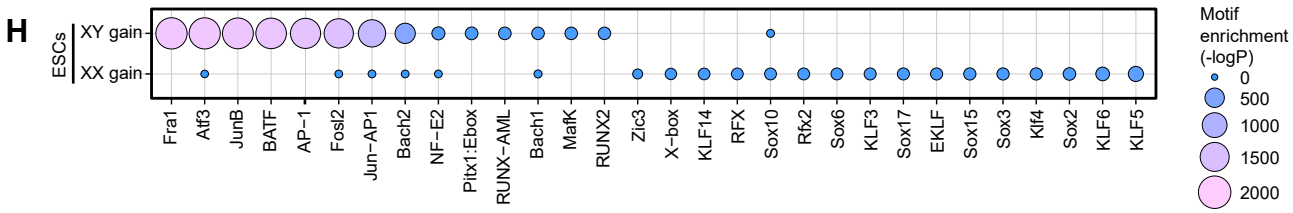

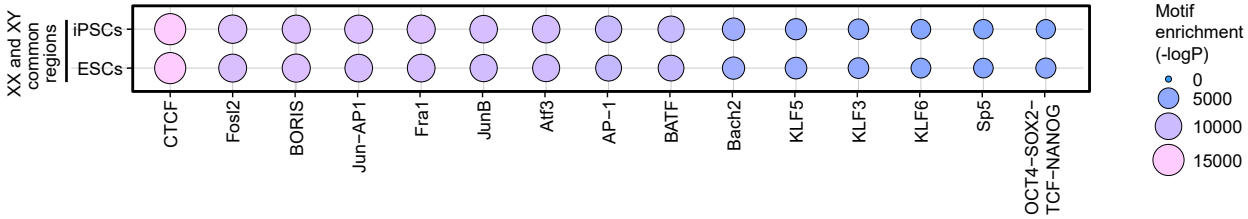

Figure S3

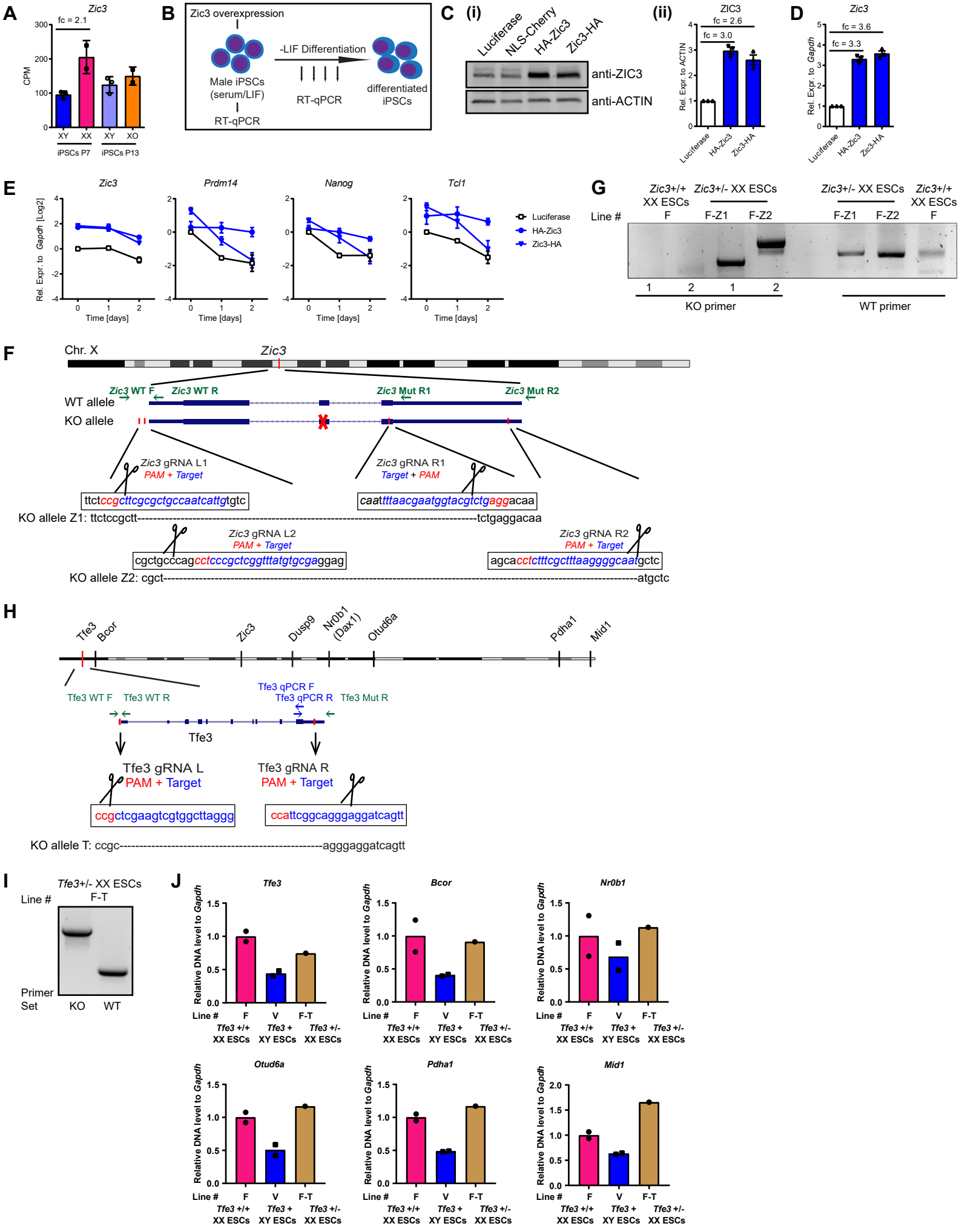
A
Zic3
fc = 2.1
CPM
XY
XX
XY
XO
iPSCs P7
iPSCs P13
B
Zic3 overexpression
Male iPSCs (serum/LIF)
-LIF Differentiation
RT-qPCR
differentiated iPSCs
RT-qPCR
C (i)
Luciferase
NLS-Cherry
HA-Zic3
Zic3-HA
anti-ZIC3
anti-ACTIN
(ii)
ZIC3
fc = 2.6
fc = 3.0
Rel. Expr. to ACTIN
Luciferase
HA-Zic3
Zic3-HA
D
Zic3
fc = 3.6
fc = 3.3
Rel. Expr. to Gapdh
Luciferase
HA-Zic3
Zic3-HA
E
Zic3
Prdm14
Nanog
Tcl1
Rel. Expr. to Gapdh [Log2]
Time [days]
Luciferase
HA-Zic3
Zic3-HA
G
Line #
Zic3+/+ XX ESCs
Zic3+/- XX ESCs
F
F-Z1
F-Z2
Zic3+/- XX ESCs
Zic3+/+ XX ESCs
F-Z1
F-Z2
F
1
2
1
2
KO primer
WT primer
F
Chr. X
Zic3
Zic3 WT F
Zic3 WT R
Zic3 Mut R1
Zic3 Mut R2
WT allele
KO allele
Zic3 gRNA L1
PAM + Target
Zic3 gRNA R1
Target + PAM
ttctccgcttcgcgctgccaatcattgtgtc
caatttttaacgaatggtacgtctgaggacaa
KO allele Z1: ttctccgctt----------tctgaggacaa
Zic3 gRNA L2
PAM + Target
Zic3 gRNA R2
PAM + Target
cgctgcccagcctcccgctcggtttatgtgcgaggag
agcacctctttcgctttaaggggcaatgctc
KO allele Z2: cgct----------atgctc
H
Tfe3
Bcor
Zic3
Dusp9
Nr0b1 (Dax1)
Otud6a
Pdha1
Mid1
Tfe3 WT F
Tfe3 WT R
Tfe3 qPCR F
Tfe3 qPCR R
Tfe3 Mut R
Tfe3
Tfe3 gRNA L
PAM + Target
Tfe3 gRNA R
PAM + Target
ccgctcgaagtcgtggcttaggg
ccattcggcagggaggatcagtt
KO allele T: ccgc----------agggaggatcagtt
I
Tfe3+/- XX ESCs
Line #
F-T
Primer Set
KO
WT
J
Tfe3
Bcor
Nr0b1
Otud6a
Pdha1
Mid1
Relative DNA level to Gapdh
Line #
F
V
F-T
Tfe3 +/+ XX ESCs
Tfe3 + XY ESCs
Tfe3 +/- XX ESCs

Figure S4

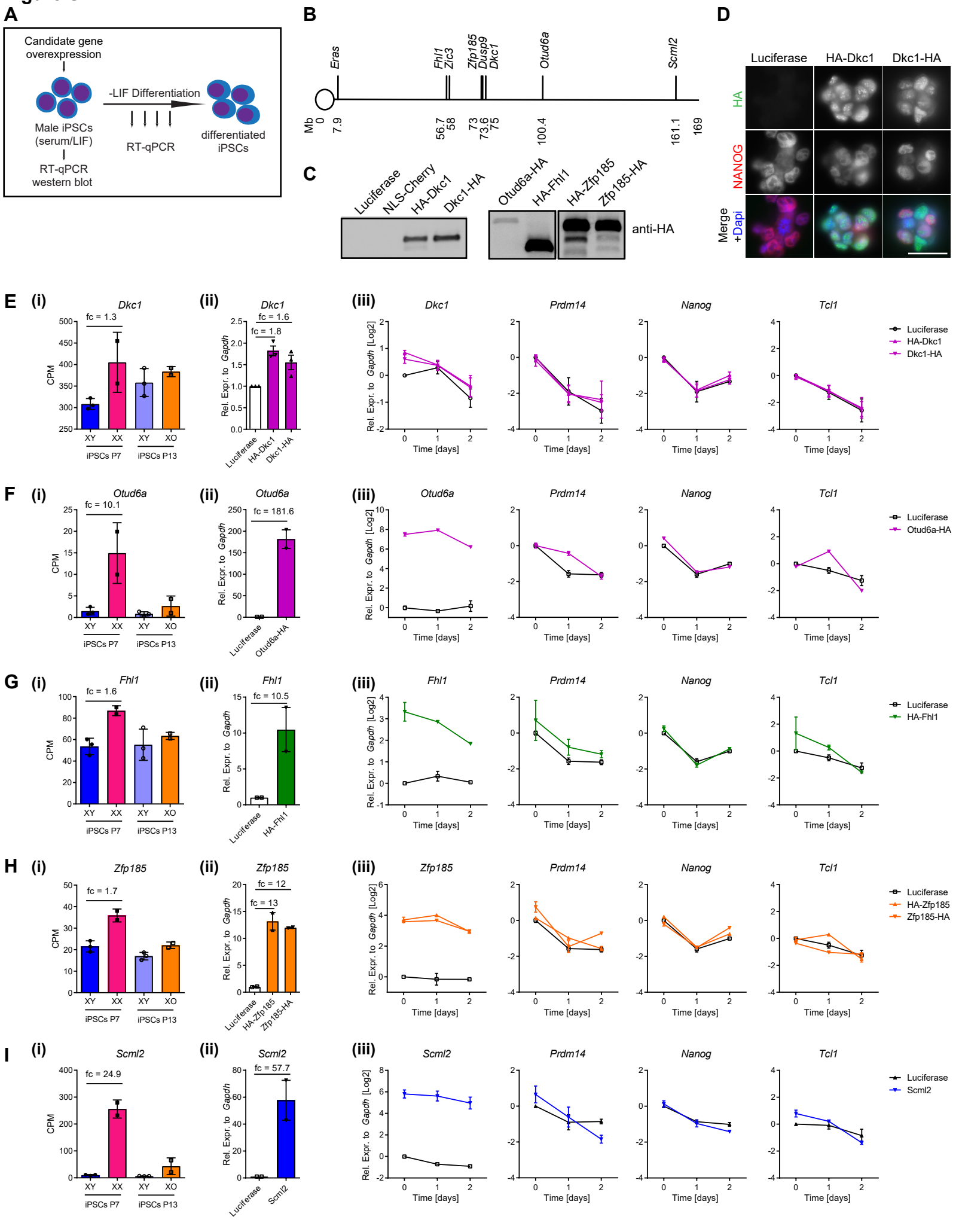
A
Candidate gene overexpression
Male iPSCs (serum/LIF)
RT-qPCR western blot
-LIF Differentiation
RT-qPCR
differentiated iPSCs
B
Eras
Fhl1 Zic3
Zfp185 Dusp9 Dkc1
Otud6a
Scml2
Mb
0
7.9
56.7 58
73 73.6 75
100.4
161.1 169
C
Luciferase
NLS-Cherry
HA-Dkc1
Dkc1-HA
Otud6a-HA
HA-Fhl1
HA-Zfp185
Zfp185-HA
anti-HA
D
Luciferase
HA-Dkc1
Dkc1-HA
HA
NANOG
Merge +Dapi
E
(i) Dkc1
fc = 1.3
CPM
XY XX XY XO
iPSCs P7 iPSCs P13
(ii) Dkc1
fc = 1.6
fc = 1.8
Rel. Expr. to Gapdh
Luciferase HA-Dkc1 Dkc1-HA
(iii) Dkc1 Prdm14 Nanog Tcl1
Rel. Expr. to Gapdh [Log2]
Time [days]
Luciferase
HA-Dkc1
Dkc1-HA
F
(i) Otud6a
fc = 10.1
(ii) Otud6a
fc = 181.6
Luciferase Otud6a-HA
(iii) Otud6a Prdm14 Nanog Tcl1
Luciferase
Otud6a-HA
G
(i) Fhl1
fc = 1.6
(ii) Fhl1
fc = 10.5
Luciferase HA-Fhl1
(iii) Fhl1 Prdm14 Nanog Tcl1
Luciferase
HA-Fhl1
H
(i) Zfp185
fc = 1.7
(ii) Zfp185
fc = 12
fc = 13
Luciferase HA-Zfp185 Zfp185-HA
(iii) Zfp185 Prdm14 Nanog Tcl1
Luciferase
HA-Zfp185
Zfp185-HA
I
(i) Scml2
fc = 24.9
(ii) Scml2
fc = 57.7
Luciferase Scml2
(iii) Scml2 Prdm14 Nanog Tcl1
Luciferase
Scml2

Figure S5

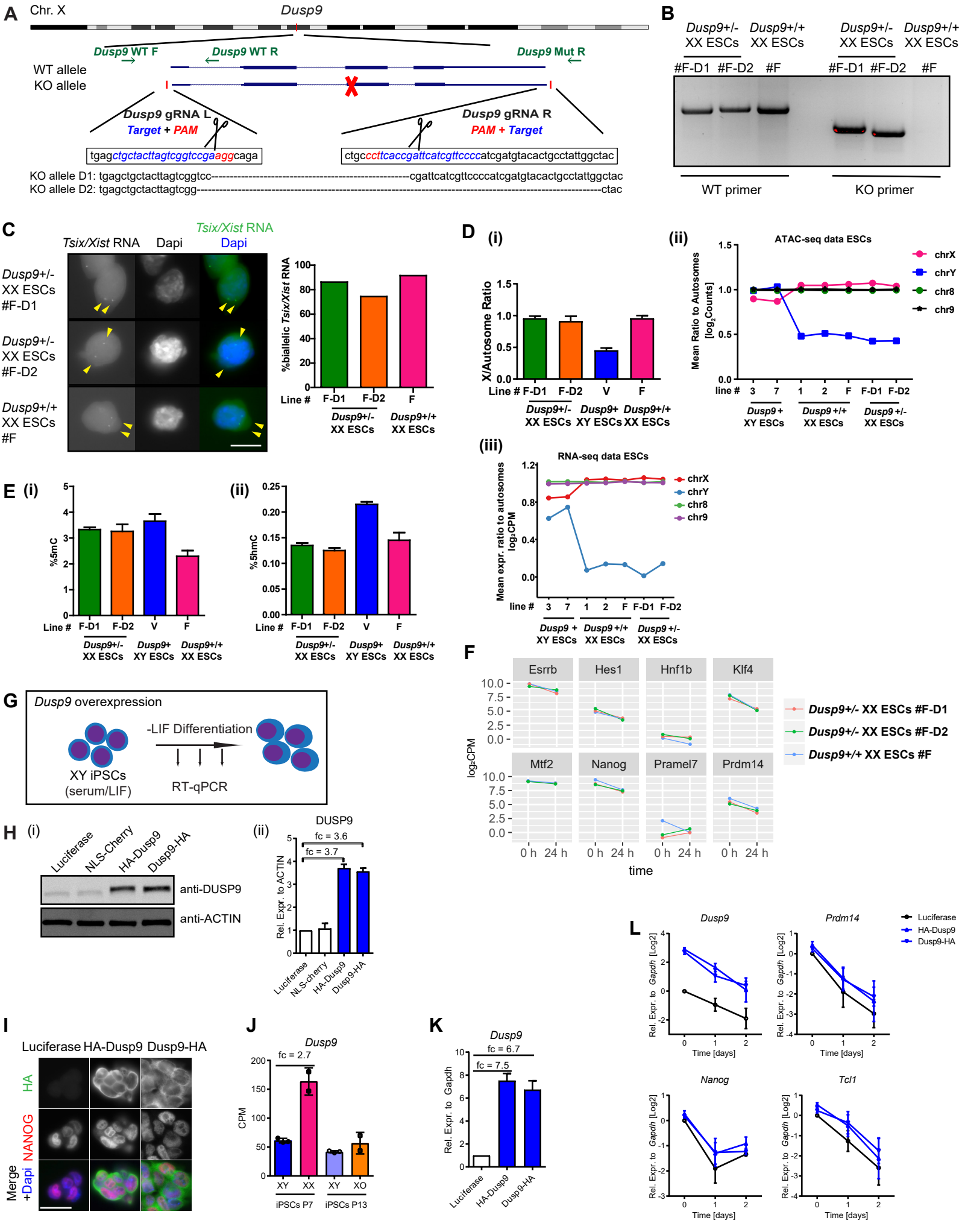
A
Chr. X
Dusp9
Dusp9 WT F
Dusp9 WT R
Dusp9 Mut R
WT allele
KO allele
Dusp9 gRNA L
Target + PAM
Dusp9 gRNA R
PAM + Target
tgagctgctacttagtcggtccgaaggcaga
ctgccttcaccgattcatcgttccccatcgatgtacactgcctattggctac
KO allele D1: tgagctgctacttagtcggtcc----------cgattcatcgttccccatcgatgtacactgcctattggctac
KO allele D2: tgagctgctacttagtcgg----------ctac
B
Dusp9+/- XX ESCs
Dusp9+/+ XX ESCs
#F-D1 #F-D2 #F
WT primer
KO primer
C
Tsix/Xist RNA
Dapi
Dusp9+/- XX ESCs #F-D1
Dusp9+/- XX ESCs #F-D2
Dusp9+/+ XX ESCs #F
%biallelic Tsix/Xist RNA
Line # F-D1 F-D2 F
Dusp9+/- XX ESCs
Dusp9+/+ XX ESCs
D (i)
X/Autosome Ratio
Line # F-D1 F-D2 V F
Dusp9+/- XX ESCs
Dusp9+ XY ESCs
Dusp9+/+ XX ESCs
(ii)
ATAC-seq data ESCs
Mean Ratio to Autosomes [log2Counts]
chrX
chrY
chr8
chr9
line # 3 7 1 2 F F-D1 F-D2
Dusp9 + XY ESCs
Dusp9 +/+ XX ESCs
Dusp9 +/- XX ESCs
(iii)
RNA-seq data ESCs
Mean expr. ratio to autosomes log2CPM
E (i)
%5mC
Line # F-D1 F-D2 V F
(ii)
%5hmC
F
Esrrb
Hes1
Hnf1b
Klf4
Mtf2
Nanog
Pramel7
Prdm14
log2CPM
0 h 24 h
time
Dusp9+/- XX ESCs #F-D1
Dusp9+/- XX ESCs #F-D2
Dusp9+/+ XX ESCs #F
G
Dusp9 overexpression
XY iPSCs (serum/LIF)
-LIF Differentiation
RT-qPCR
H (i)
Luciferase
NLS-Cherry
HA-Dusp9
Dusp9-HA
anti-DUSP9
anti-ACTIN
(ii)
DUSP9
fc = 3.6
fc = 3.7
Rel. Expr. to ACTIN
I
Luciferase HA-Dusp9 Dusp9-HA
HA
NANOG
Merge +Dapi
J
Dusp9
fc = 2.7
CPM
XY XX XY XO
iPSCs P7 iPSCs P13
K
Dusp9
fc = 6.7
fc = 7.5
Rel. Expr. to Gapdh
L
Dusp9
Prdm14
Nanog
Tcl1
Rel. Expr. to Gapdh [Log2]
Time [days]
Luciferase
HA-Dusp9
Dusp9-HA

Figure S6

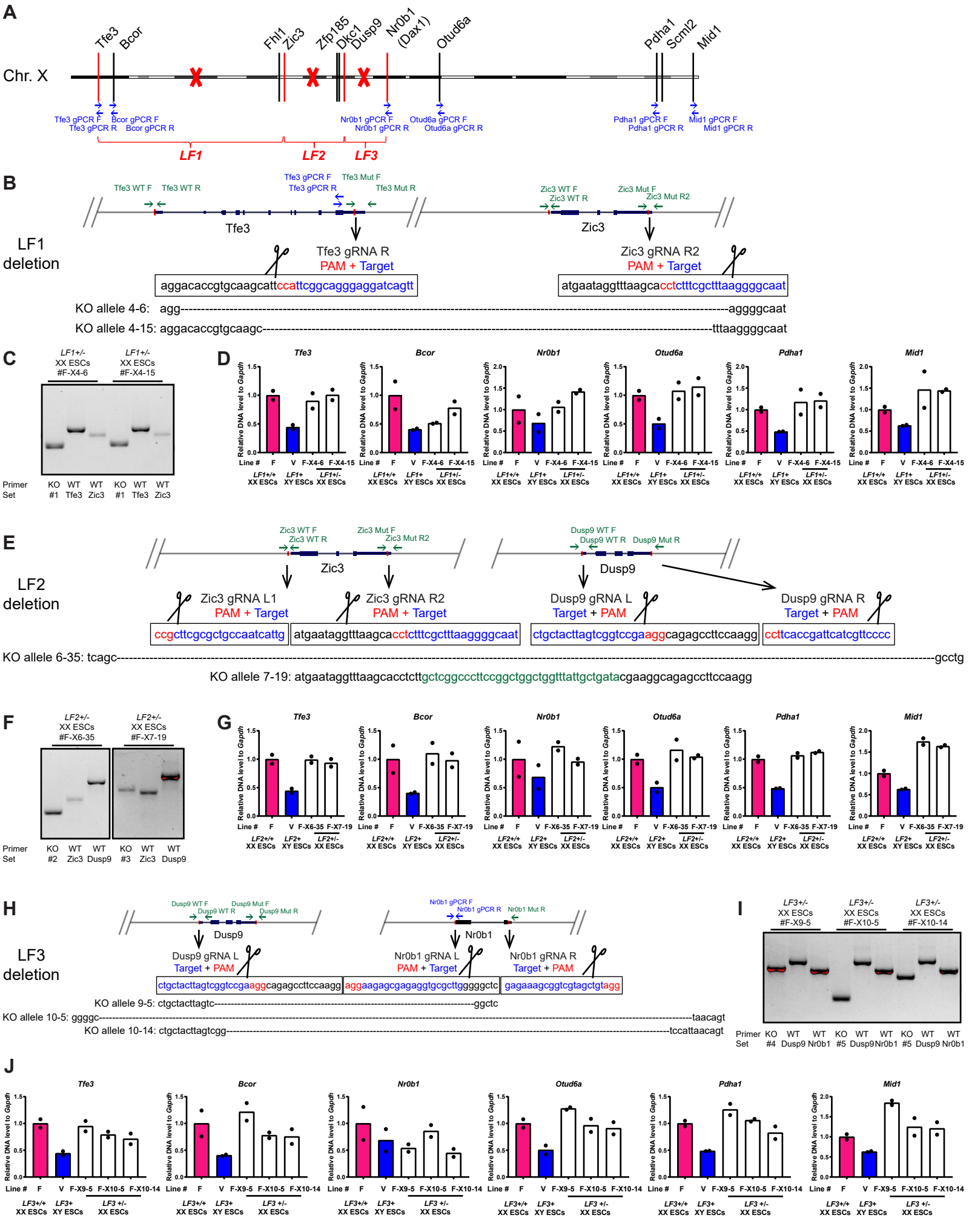
A
Chr. X
Tfe3
Bcor
Fhl1
Zic3
Zfp185
Dkc1
Dusp9
Nr0b1 (Dax1)
Otud6a
Pdha1
Scml2
Mid1
Tfe3 gPCR F
Tfe3 gPCR R
Bcor gPCR F
Bcor gPCR R
Nr0b1 gPCR F
Nr0b1 gPCR R
Otud6a gPCR F
Otud6a gPCR R
Pdha1 gPCR F
Pdha1 gPCR R
Mid1 gPCR F
Mid1 gPCR R
LF1
LF2
LF3
B
LF1 deletion
Tfe3 WT F
Tfe3 WT R
Tfe3 gPCR F
Tfe3 gPCR R
Tfe3 Mut F
Tfe3 Mut R
Zic3 WT F
Zic3 WT R
Zic3 Mut F
Zic3 Mut R2
Tfe3
Zic3
Tfe3 gRNA R
PAM + Target
Zic3 gRNA R2
PAM + Target
aggacaccgtgcaagcattccattcggcagggaggatcagtt
atgaataggtttaagcacctctttcgctttaaggggcaat
KO allele 4-6: agg----------aggggcaat
KO allele 4-15: aggacaccgtgcaagc----------tttaaggggcaat
C
LF1+/- XX ESCs #F-X4-6
LF1+/- XX ESCs #F-X4-15
Primer Set
KO #1
WT Tfe3
WT Zic3
KO #1
WT Tfe3
WT Zic3
D
Tfe3
Bcor
Nr0b1
Otud6a
Pdha1
Mid1
Relative DNA level to Gapdh
Line #
F
V
F-X4-6
F-X4-15
LF1+/+ XX ESCs
LF1+ XY ESCs
LF1+/- XX ESCs
E
LF2 deletion
Zic3 WT F
Zic3 WT R
Zic3 Mut F
Zic3 Mut R2
Dusp9 WT F
Dusp9 WT R
Dusp9 Mut R
Zic3
Dusp9
Zic3 gRNA L1
PAM + Target
Zic3 gRNA R2
PAM + Target
Dusp9 gRNA L
Target + PAM
Dusp9 gRNA R
Target + PAM
ccgcttcgcgctgccaatcattg
atgaataggtttaagcacctctttcgctttaaggggcaat
ctgctacttagtcggtccgaaggcagagccttccaagg
ccttcaccgattcatcgttcccc
KO allele 6-35: tcagc----------gcctg
KO allele 7-19: atgaataggtttaagcacctcttgctcggcccttccggctggctggtttattgctgatacgaaggcagagccttccaagg
F
LF2+/- XX ESCs #F-X6-35
LF2+/- XX ESCs #F-X7-19
Primer Set
KO #2
WT Zic3
WT Dusp9
KO #3
WT Zic3
WT Dusp9
G
LF2+/+ XX ESCs
LF2+ XY ESCs
LF2+/- XX ESCs
F-X6-35
F-X7-19
H
LF3 deletion
Dusp9 WT F
Dusp9 WT R
Dusp9 Mut F
Dusp9 Mut R
Nr0b1 gPCR F
Nr0b1 gPCR R
Nr0b1 Mut R
Dusp9
Nr0b1
Dusp9 gRNA L
Target + PAM
Nr0b1 gRNA L
PAM + Target
Nr0b1 gRNA R
Target + PAM
ctgctacttagtcggtccgaaggcagagccttccaagg
aggaagagcgagaggtgcgcttgggggctc
gagaaagcggtcgtagctgtagg
KO allele 9-5: ctgctacttagtc----------ggctc
KO allele 10-5: ggggc----------taacagt
KO allele 10-14: ctgctacttagtcgg----------tccattaacagt
I
LF3+/- XX ESCs #F-X9-5
LF3+/- XX ESCs #F-X10-5
LF3+/- XX ESCs #F-X10-14
Primer Set
KO #4
WT Dusp9
WT Nr0b1
KO #5
WT Dusp9
WT Nr0b1
KO #5
WT Dusp9
WT Nr0b1
J
F-X9-5
F-X10-5
F-X10-14
LF3+/+ XX ESCs
LF3+ XY ESCs
LF3 +/- XX ESCs

Figure S7

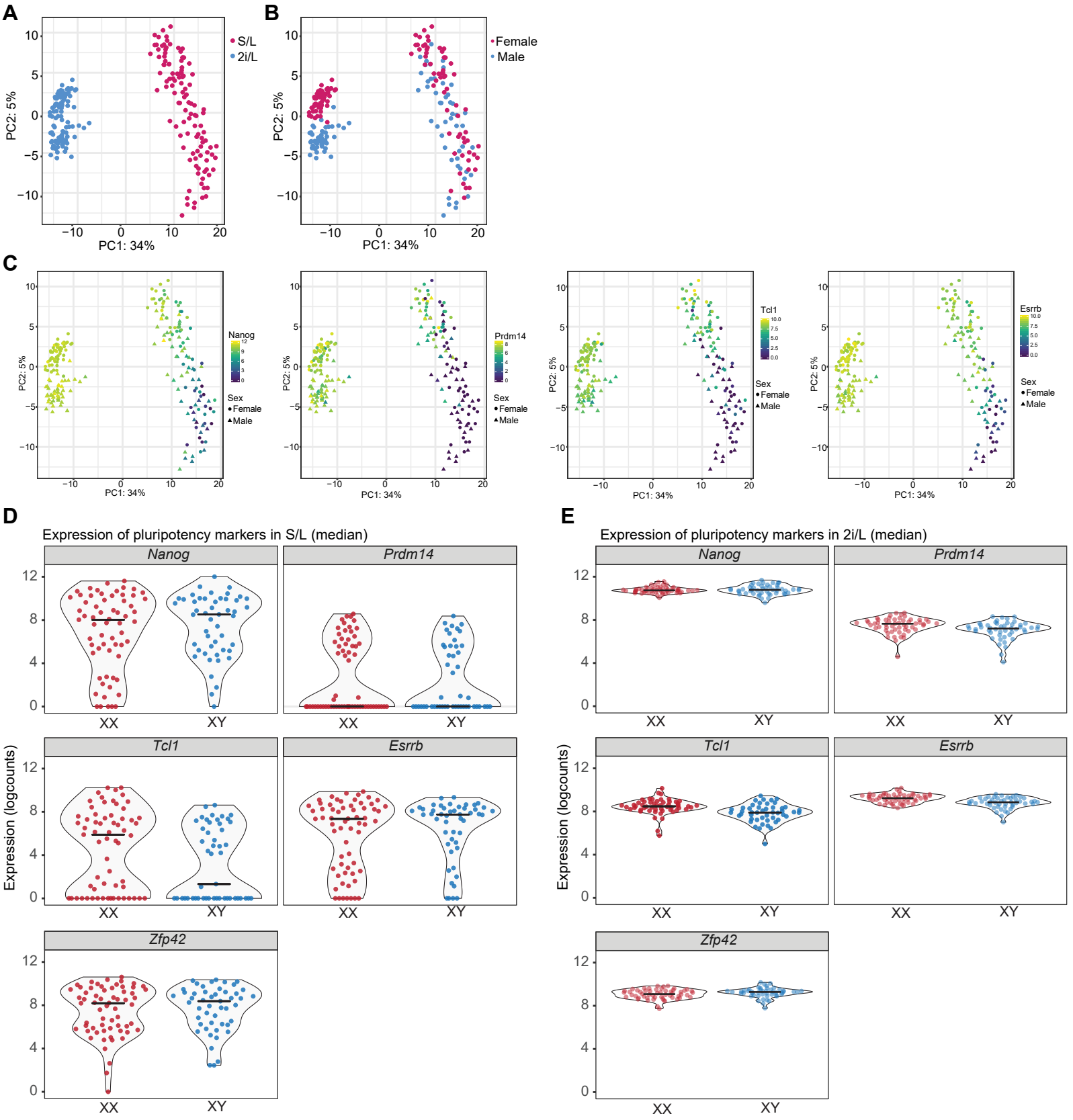
A
B
C
D
E
S/L
2i/L
Female
Male
PC1: 34%
PC2: 5%
Nanog
Prdm14
Tcl1
Esrrb
Sex
Female
Male
Expression of pluripotency markers in S/L (median)
Expression of pluripotency markers in 2i/L (median)
Expression (logcounts)
Zfp42
XX
XY

SUPPLEMENTAL FIGURES AND LEGENDS

Figure S1. X-dosage-specific differences in transcriptome, pluripotency exit and cell growth in mouse iPSCs. Related to Figure 1.

(A) Immunofluorescence analysis for NANOG and DPPA4 in iPSCs and ESCs grown in 2i/L. MEFs served as negative control. Representative images for NANOG (Red), DPPA4 (Green) and Dapi (Blue, nuclei counterstaining) are shown. Scale bar, 50 μm.
(B) Summary of ESC and iPSC lines used in this study as well as NANOG and DPPA4 protein expression analysis in 2i/L and in S/L.
(C) (i) PCA of our own RNA-seq data for XX and XY iPSCs, XY ESCs (V6.5), as well as published RNA-seq for XY ESCs (V6.5, (Chronis et al., 2017)) and somatic MEFs. (ii) Representative image of adult male chimeric mice (left) and germline transmitted pup (right) produced from XY ESCs (V6.5).
(D) RNA FISH analysis for *Tsix/Xist* expression in iPSCs grown in 2i/L. Representative images for *Tsix/Xist* RNA (Green) and Dapi (Blue, nuclei counterstaining) are shown. Yellow arrowheads point to *Tsix/Xist* transcriptional sites. Also see (Pasque et al., 2018). Scale bar, 10 μm. Right: Quantification of *Tsix/Xist* RNA FISH signal from Figure S1C and for all lines, plotted as the proportion of cells with biallelic *Tsix/Xist* signal (= number of cells with biallelic *Tsix/Xist* expression / number of cells with biallelic or monoallelic expression). The number of counted nuclei is > 50 per cell line.
(E) qPCR analysis for X-chromosome DNA copy number in both early passage and late passage iPSCs grown in S/L. X copy number are presented as the average ratio of gDNA quantities for four X-linked genes (*Tfe3, Bcor, Pdha1, and Mid1,* locations in X-chromosome shown in lower panel) to gDNA quantities for autosomal gene *Gapdh*.
(F) Karyotype analysis of iPSC lines grown in S/L. + mar denotes chromosomal fragment of unknown origin.
(G) Unsupervised hierarchical clustering of stem-cell maintenance gene expression in XX, XY and XO iPSCs.
(H) RT-qPCR analysis for pluripotency-associated gene expression in XX, XY and XO iPSCs grown in S/L. The expression values are represented as averages (±SEM) of XY, XX and XO iPSC lines (three different lines each) in early passage (P8) and late passage (P14), respectively. Statistical significance was analysed using the unpaired, two-tailed t-test (**p<0.01).
(I) DEG analysis, identifying clear differences between XX and XY ESCs.
(J) Venn diagrams showing the overlap between XX vs XY iPSCs DEGs and XX vs XY ESCs DEGs. Despite difference in genetic background between iPSCs and ESCs, 93 genes are differentially expressed between XX and XY cells both for iPSCs and ESCs.
(K) RT-qPCR for pluripotency-associated genes for individual XY (blue), XX (magenta) and pXO (orange, line 26) iPSC lines undergoing EpiLC differentiation.
(L) Unsupervised hierarchical clustering of XX, XY and XO iPSC and ESC lines based on expression of X-linked genes in undifferentiated state (i), and pluripotency-associated genes in undifferentiated state (ii) and 24h of LIF withdrawal differentiated state (iii).
(M) Growth curves and doubling times of XY and XX iPSCs (i) and ESCs (ii) in 2i/LIF condition. Cell counts were obtained at different time points, as indicated. Cell counts are shown as fold changes relative to 0h and represent the averages cell count (±SEM) over three cell lines each for XY and XX iPSCs (n=1, left panel) at early passage (P8) and over two lines each for two XY and XX ESCs (n=1, right panel). Growth curve: *p* value <0.001 (***) between XY and XX cell lines, by two-way repeated-measures ANOVA with Bonferroni posttests. Td: *p<0.05, XY lines vs XX lines, by unpaired two-tailed t-test.
(N) (i) EdU incorporation in combination with DNA staining using PI shows a higher number of XX iPSCs residing in S phase, and a lower number of XX iPSCs residing in G1 phase when compared to XY iPSCs. Results show the averages (±SEM) over three XX female iPSC lines and three XY male iPSC lines (n=1). Significance was tested using one-way ANOVA with Sidak's multiple comparisons test (**p<0.01, ***p<0.001). (ii) FUCCI reporter expression shows the number of XX female ESCs activating the G1 phase reporter is lower than that of XY male ESCs, and the number of XX female ESCs activating the S/G2/M phase reporter is higher than that of XY male ESCs. Results show the averages (±SEM) over two XX female and two XY male FUCCI reporter ESC lines (n=1). Significance was tested using one-way ANOVA with Bonferroni's multiple comparisons test (**p<0.01, ***p<0.001).
(O) XY and XX ESCs competition assay. WT XX ESCs were mixed with GFP-labelled XY ESCs (Oct4-GiP) in different ratios (left panel, scheme of the experiment) and the proportion of GFP-labeled cells in the culture was

measured over time (n=2), as indicated. *p<0.05, **p <0.01, by two-way repeated-measures ANOVA with Dunnett's multiple comparisons test compared to day 0.

Figure S2. Influence of X-dosage on the chromatin regulatory landscape of mouse iPSCs and ESCs. Related to Figure 2 and Figure 3.

(A) Distance to closest TSSs of "Not differentially accessible", "XX gain" and "XY gain" ATAC-seq regions in iPSCs.
(B) Mean read count ratio to autosomes showing which lines have increased/decreased ATAC-seq reads on the Y chromosome, X chromosome, chromosome 8 and chromosome 9. This analysis confirms the higher abundance of DNA sequence reads coming from the Y chromosome in XY lines, and from the X chromosome in XX lines.
(C) Sample-to-sample distance heatmap showing the Euclidean distances (calculated from the rlog transformed counts, DESeq2) between ESCs samples. Samples cluster by X-dosage (XX vs XY).
(D) Differential chromatin accessibility analysis between XX and XY ESCs. Log2 fold change (XX/XY) in reads per accessible region are plotted against the mean reads per ATAC-seq peak. Thousands of open chromatin regions that more open in XX ESCs or in XY ESCs (|log2fold|>=1, false discovery rate (FDR)<=0.05).
(E) Venn diagrams showing the overlap between genes nearest to the "XX gain" or "XY gain" regions defined in (D) and the DEGs between XX and XY ESCs (DEGs= $|\log_2 fold| >= \log_2 1.5$, FDR<=0.05).
(F) Transcription factor motifs enriched in chromatin regions more open in XX ESCs.
(G) Transcription factor motifs enriched in chromatin regions more open in XY ESCs.
(H) Overview of motif enrichment in XX gain and XY gain chromatin regions in ESCs.
(I) Overview of motif enrichment in open chromatin not differentially accessbilie between XX and XY cells in both ESCs and iPSCs.
(J) Transcription factor motifs enriched in open chromatin not differentially accessbilie between XX and XY iPSCs.

Figure S3. Effects of Zic3 overexpression and Zic3/ Tfe3 heterozygous deletion in XX ESCs on pluripotency exit. Related to Figure 4.

(A) Expression of *Zic3* in XY, XX and XO iPSCs showing 2.1 fold increased *Zic3* dosage in XX iPSCs over XY and XO iPSCs as assessed by RNA-seq.
(B) Scheme of *Zic3* overexpression in XY iPSCs, followed by characterization and LIF withdrawal differentiation.
(C) (i) Western blot analysis for ZIC3 and ACTIN in XY iPSCs after HA-Zic3 or Zic3-HA overexpression. (ii) Quantification using ACTIN as loading control. ZIC3 protein values are represented as averages (±SEM) of three independent experiments.
(D) RT-qPCR of *Zic3* in HA-tagged Zic3 overexpressing (3.3-3.6 fold) XY iPSCs. XY iPSCs overexpressing Luciferase served as negative control. Results are presented as averages (±SEM) of three independent experiments.
(E) RT-qPCR analysis for *Zic3*, *Prdm14*, *Nanog* and *Tcl1* expression during LIF withdrawal in XY iPSCs overexpressing HA-Zic3, Zic3-HA or Luciferase control. Results are presented as averages (±SEM) of three independent experiments (n=3).
(F) Scheme of heterozygous *Zic3* deletion strategy in XX ESCs. The sequences of the gRNAs used to deleted *Zic3* are shown in blue with PAM sequences in red. Two independent *Zic3*+/- XX ESC lines were derived. The sequences of the knockout (KO) alleles were obtained by Sanger sequencing. Red line shows the location of the gRNAs. Green arrows shows the locations of the primers for genotyping PCR.
(G) Genotyping of *Zic3* heterozygous deleted XX ESC lines for both WT and KO alleles. The parental *Zic3*+/+ ESCs were used as positive control for the WT allele and as negative control for the KO allele.
(H) as in (F) but for heterozygous *Tfe3* deletion strategy in XX ESCs.
(I) Genotyping of *Tfe3* heterozygous deleted XX ESC lines for both WT and KO alleles.
(J) qPCR analysis for X-chromosome DNA copy number. X copy number are presented as the relative gDNA quantities for six X-linked genes (*Tfe3, Bcor, Nr0b1, Otud6a, Pdha1, and Mid1,* locations in X-chromosome shown in Figure S3H) to gDNA quantities for autosomal gene *Gapdh*.

Figure S4. Overexpression of X-linked candidates Dkc1, Otud6a, Fhl1, Zfp185 and Scml2 has no effect on the pluripotency exit kinetics of XY iPSCs. Related to Figure 4.

(A) Scheme for candidate X-linked gene overexpression in XY iPSCs, followed by LIF withdrawal.
(B) Map of the X-chromosome showing candidate X-linked genes.

(C) Western blot analysis for HA-tagged DKC1, OTUD6A, FHL1, ZFP185 using an anti-HA antibody. ACTIN was used as a loading control. Representative images are shown.
(D) Immunofluorescence analysis for NANOG and HA in stable XY iPSC lines overexpressing HA-tagged *Dkc1*. The stable XY iPSC line overexpressing Luciferase was used as a negative control. Representative images for NANOG (Red), HA (Green) and Dapi (Blue, nuclei counterstaining) are shown. Scale bar, 50 μm.
(E-I) (i) Expression of X-linked candidates *Dkc1, Otud6a, Fhl1, Zfp185 and Scml2* in XY, XX and XO iPSCs showing fold change (fc) in XX iPSCs over XY iPSCs as assessed by RNA-seq. **(ii)** RT-qPCR of X-linked candidates expression in XY iPSC lines with ectopic expression of HA-tagged *Dkc1* (E), HA-tagged *Otud6a* (F), HA-tagged *Fhl1* (G), HA-tagged *Zfp185* (H) or *Scml2* (I). XY iPSCs overexpressing Luciferase served as negative control. **(iii)** RT-qPCR for pluripotency-associated genes *Prdm14, Nanog* and *Tcl1,* and the respective X-linked candidate genes in XY iPSC lines stably overexpressing the respective HA-tagged X-linked candidates and subjected to LIF withdrawal. Results are presented as averages (±SEM) of three (E) or two (F-J) independent experiments, which are not statistically significant by two-way repeated-measures ANOVA with Bonferroni posttests.

Figure S5. Characterization of Dusp9 heterozygous mutant XX female ESCs. Related to Figure 5.

(A) Scheme of heterozygous *Dusp9* deletion in XX ESCs. The gRNAs sequences used to delete the *Dusp9* gene are shown in blue with PAM sequences in red. Two independent *Dusp9*+/- ESC lines were derived. The sequences of the KO alleles were obtained by DNA Sanger sequencing. Red line shows the location of the gRNAs. Green arrows shows the locations of the primers for genotyping PCR.
(B) Genotyping *Dusp9*+/- ESC lines for both the WT and the KO allele. The parental XX ESC line was used as a positive control for the WT allele PCR and as a negative control for the KO allele PCR.
(C) RNA FISH analysis for *Tsix/Xist* expression in the two independent *Dusp9*+/- ESC lines and their parental XX ESC line. Representative images for *Tsix/Xist* RNA (Green) and Dapi (Blue, nuclei counterstaining) are shown. Yellow arrowheads point to *Tsix/Xist* transcriptional sites. Scale bar, 10 μm. Right: Quantification of Figure S5C, plotted as the proportion of cells with biallelic *Tsix/Xist* signal (= number of cells with biallelic *Tsix/Xist* expression / number of cells with biallelic or monoallelic expression). Numbers of counted nuclei > 50 per cell line.
(D) (i) qPCR analysis for X-chromosome DNA copy number. X copy number are presented as the average ratio of gDNA quantities for four X-linked genes (Tfe3, Bcor, Pdha1, and Mid1) to gDNA quantities for autosomal gene Gapdh. Results are presented as averages (±SEM) of the same lines in two independent qPCR experiments (n=2). (ii) Mean read count ratio to autosomes showing which lines have increased/decreased ATAC-seq reads on the Y chromosome, X chromosome, chromosome 8 and chromosome 9. This analysis confirms the higher abundance of DNA sequence reads coming from the Y chromosome in XY lines, and from the X chromosome in XX lines. (iii) Mean expression ratio to autosomes for sex chromosomes and chromosomes 8 and 9.
(E) DNA methylation analysis of *Dusp9*+/- ESCs, *Dusp9*+/+ ESCs and XY ESCs by mass spectrometry. (i) 5mC, (ii) 5hmC.
(F) RNA-seq analysis of pluripotency associated gene expression during pluripotency exit in Dusp9+/- and Dusp9+/+ ESCs. The delay in pluripotency gene downregulation is maintained.
(G) Scheme of *Dusp9* overexpression in male iPSCs grown in S/L, followed by characterization and LIF withdrawal.
(H) (i) Western blot analysis for DUSP9 in XY iPSC lines with ectopic HA-tagged DUSP9 expression. ACTIN was used as a loading control. (ii) quantification using ACTIN as loading control. DUSP9 protein values are represented as averages (±SEM) of three independent experiments (n=3).
(I) Immunofluorescence analysis for NANOG and HA-tagged DUSP9 in stable male iPSCs with HA-tagged DUSP9 overexpression. The stable male iPSC line overexpressing Luciferase was used as a negative control. Representative images for NANOG (Red), HA (Green) and Dapi (Blue, nuclei counterstaining) are shown. Scale bar, 50 μm.
(J) Expression of *Dusp9* in XX, XY and XO iPSCs showing 2.7 fold increased *Dusp9* dosage in XX iPSCs over XY and XO iPSCs as assessed by RNA-seq.
(K) qRT-PCR for *Dusp9* in XY iPSCs overexpressing HA-Dusp9, Dusp9-HA and control Luciferase.
(L) qRT-PCR for *Dusp9* and pluripotency-associated genes *Prdm14*, *Nanog* and *Tcl1* in XY iPSCs overexpressing *Dusp9* following LIF withdrawal. The stable XY iPSC line overexpressing Luciferase served as a negative control. Results are presented as averages (±SEM) of three independent experiments.

Figure S6. Large fragment heterozygous deletion of X chromosome in XX ESCs. Related to Figure 6.

(A) Scheme of the three large fragment (LF) heterozygous deletions in XX female ESCs.

(B) Scheme of heterozygous LF1 deletion in XX ESCs. The gRNAs sequences are shown in blue with PAM sequences in red. Two independent *LF1*+/- ESC lines were derived. The sequences of the KO alleles were obtained by DNA Sanger sequencing. Red line shows the location of the gRNAs. Green arrows shows the locations of the primers for genotyping PCR used in (C).
(C) Genotyping *LF1*+/- XX ESC lines for both the WT and the KO allele.
(D) qPCR analysis for X-chromosome DNA copy number. X copy number are presented as the relative gDNA quantities for six X-linked genes (Tfe3, Bcor, Pdha1, and Mid1) to gDNA quantities for autosomal gene Gapdh. Results are presented as averages (±SEM) of the same lines in two independent qPCR experiments (n=2).
(E-G) As in (B-D) for heterozygous LF2 deletion in XX ESCs. Two independent *LF2*+/- ESC lines were derived and validated.
(H-J) As in (B-D) for heterozygous LF3 deletion in XX ESCs. Three independent *LF3*+/- ESC lines were derived and validated.

Figure S7. Single cell RNA-seq analysis of XX female and XY male ESCs in S/L and 2i/L.

(A) PCA analysis of XX female and male XY ESCs S/L and 2i/L single cell RNA-seq data from (Chen et al., 2016a). Cells grown in S/L are shown in magenta, those grown in 2i/L are shown in blue.
(B) Same analysis as in (A), showing XX female ESCs in magenta and XY male ESCs in blue.
(C) Expression of *Nanog*, *Prdm14*, *Esrrb* and *Tcl1* projected onto the PCA shown in (A) and (B).
(D) Expression (log read count) of pluripotency associated genes *Nanog*, *Prdm14*, *Tcl1*, *Esrrb* and *Zfp42* in single XX female and XY male ESCs grown in S/L. Violin plots indicate the distribution of single cells where each dot is a cell. Black lines indicate median gene expression.
(E) As in (D) for the same cells grown in 2i/L.

SUPPLEMENTAL TABLES

Table S1. Summary of cell lines used in this study.

Table S2. Differentially expressed genes between XX and XY iPSCs (ESCs). Related to Figure 1F and S1I respectively.

Table S3. Differentially accessible regions between XX and XY iPSCs (ESCs), and the association with differential gene expression. Related to Figure 2B/C/F, S2D/E.

Table S4 Expression level of X-linked candidate genes in XX and XY iPSCs and ESCs. Related to Figure 4A, 5, S3-5.

Table S5. Primer sequences.

SUPPLEMENTAL EXPERIMENTAL PROCEDURES

Mice and reprogramming

MEFs were isolated from individual E14.5 mouse embryos obtained from a cross between wild type (WT) C57BL/6 and homozygous Rosa26:M2rtTA, TetO-OSKM mice (Carey et al., 2010). Individual embryos were genotyped for sex using *Ube1* as previously described (See S9 Table for primer sequence) (Pasque et al., 2014) using homemade Taq DNA Polymerase and grown in MEF medium [DMEM (Gibco, 41966-052) supplemented with 10% (v/v) fetal bovine serum (FBS, Gibco, 10270-106), 1% (v/v) penicillin/streptomycin (P/S, Gibco, 15140-122), 1% (v/v) GlutaMAX (Gibco, 35050-061), 1% (v/v) non-essential amino acids (NEAA, Gibco, 11140-050), and 0.8% (v/v) beta-mercaptoethanol (Sigma, M7522)]. Reprogramming was induced by doxycycline (final 2 µg/ml) in mouse ESC medium [KnockOut DMEM (Gibco, 10829-018) supplemented with 15% FBS, 1% (v/v) P/S, 1% (v/v) GlutaMAX, 1% (v/v) NEAA, 0.8% (v/v) beta-mercaptoethanol, and mouse LIF] in the presence of ascorbic acid (final 50 µg/ml). Individual colonies were picked at day 16 onto irradiated male feeders in ESC medium without doxycycline or ascorbic acid and expanded for three passages, eventually obtaining 10 female iPSC lines (lines 1, 4, 5, 6, 8, 12, 13,

14, 16, 17, 18) and 11 male iPSC lines (lines 19, 20, 21, 22, 23, 24, 25, 26, 27, 28, 29) at passage (P) 4 (S1 Fig B). iPSC lines 1, 4, 8, 12, 14, 16, 20, 21, 22, 24, 26 and 28 were also used in another study (Pasque et al., 2018) (S1 Table). Mus/Cas ESCs were isolated from E3.5 embryos resulting from a cross between Cast/Eij males and C57B6/J females, as described (Czechanski et al., 2014). All animal work carried out in this study is covered by a project license approved by the KU Leuven Animal Ethics Committee.

Cell lines and culture

XY and XX Mus/Cas ESCs were newly derived in our lab and also obtained from the Deng laboratory (Chen et al., 2016a). XY ESCs (V6.5) and XX ESCs (F1-2-1) were obtained from the Plath laboratory. GFP-labelled (Oct4-GiP) XY ESCs were previously described (Ying et al., 2002). ESCs and iPSCs (male iPSC line 4, 8, 16; female iPSC line 20, 21, 22) were expanded on top of male WT feeders in mouse ESC medium (S/L condition), eventually early passage cells (iPSCs: P6-P8) and late passage cells (iPSCs: P13-P14) were used for further experiments. ESCs and iPSCs (male iPSC lines 1, 4, 8, 12, 16; female iPSC lines 19, 20, 21, 22, 23, 26) were adapted to 2i/LIF, where cells grown on feeders in S/L condition (iPSCs: P4) were switched to new tissue culture dishes precoated with gelatin (from porcine skin, 0.1% g/v final, Sigma, G2500) without feeders in 2i/LIF medium [N2B27 basal medium (Neurobasal medium (50% v/v final, Gibco, 21103-049) and DMEM/F-12 medium (50% final, Gibco, 11320-074) supplemented with L-Glutamine (1.25 mM final, Gibco, 25030081), NDiff Neuro2 supplement (1x final, Millipore, SCM012), B27 supplement (1x final, Gibco, 17504-044), 0.8% (v/v) beta mercapto-ethanol, and 1% (v/v) P/S) supplemented with 0.35% (g/v) Bovine Serum Albumin (BSA, Sigma, A7979), homemade mouse LIF, GSK3 inhibitor CHIR-99021 (3 μM final, Axon Medchem, Axon 1386) and MEK inhibitor PD0325901 (1 μM final, Axon Medchem, Axon 1408)] for four passages.

Plasmids Constructs

The full-length mouse cDNAs of *Dusp9, Zic3*, *Dkc1, Otud6a, Fhl1, Zfp185*, and *Luciferase* (from pGL2-Basic Promage, E1641), *NLS-cherry* was cloned into pENTR vectors (Invitrogen, K240020) with either a C-terminal or a N-terminal HA tag, or no tag, and recombined into pPB-CAG-Dest-pA-pgk-bsd (PB-DEST-BSD) destination vectors. The PB-Scml2-BSD plasmid was obtained by recombining the pDONR221-Scml2 plasmid (Branco et al., 2016) into PB-DEST-BSD. Guide RNAs (gRNAs) were cloned into SapI digested pZB-sg3 (Fulco et al., 2016). All gRNAs sequences are included in S9 Table , S3 Fig F/H, S5 Fig A and S6 Fig B/E/H. All constructs were verified by DNA Sanger sequencing.

Generation of stable male iPSCs overexpressing X-linked candidate genes

Male iPSCs (line 4, P5, grown on feeders in S/L conditions) were feeder-depleted before seeding in six-well plates precoated with 0.1% gelatin in S/L medium at a density of 650,000 cells per well, which were co-transfected with 1 ug of PB expression constructs encoding candidate genes and 3 ug of pCAGP Base (Silva et al., 2009) using 10 μl Lipofectamine 2000 (Invitrogen, 11668027). Transfected cells were selected with 20 μg/mL blasticidin (Fisher BioReagents, BP2647100) supplemented to the medium for two days starting from 24h after transfection and maintained with 5 μg/mL blasticidin thereafter.

Generation of XX female ESC lines with heterozygous deletions of X-linked candidate genes

2000,000 female F1-2-1 ESCs (P19, grown on feeders in S/L condition) were resuspended in 1 ml of S/L medium and co-transfected with 2 ug of a plasmid expressing Cas9 under a CAG promoter and 1 ug of 2 plasmids (pZB-sg3 (Fulco et al., 2016)) containing gRNAs (S9 Table) using 10 μl Lipofectamine 2000 (Invitrogen, 11668027) (S3 Fig F/H, S5 Fig A and S6 Fig B/E/H) for one hour before plating on 4-drug resistant (DR4) feeders. Transfected cells were selected with 2 μg/mL puromycin (Fisher BioReagents, BP2647100) on DR4 feeders in ESC medium for two days starting from 24h after transfection, and expanded at low density on WT feeders in 10cm dishes. Individual colonies were picked onto WT feeders, expanded for another two passages and genotyped for both WT and mutant alleles (primers in Table S8). WT and mutant alleles were further verified by DNA Sanger sequencing.

Differentiation

To induce differentiation towards epiblast-like cells (EpiLCs), ESCs and iPSCs (male lines: 1, 4, 8, 12, 16; female lines: 19, 20, 21, 22, 23, 26; P8), which had been adapted to 2i/LIF conditions for 4 passages, were plated in N2B27 basal medium supplemented with 10 ng/ml Fibroblast Growth Factor-basic (Fgf2, Peprotech, 100-18C) and 20 ng/ml Activin A (ActA, Peprotech, 120-14E) on Fibronectin (5 ug/10 cm^2, Millipore, FC010-5MG)-coated tissue culture plates at a cell density of $8*10^4$ cells/cm^2 for four days, during which medium was refreshed daily and cells were harvested at different time points (0h, 12h, 1 day, 2 days, 3 days and 4 days), as previously described (Schulz et al., 2014). ESCs (WT female and male ESCs, *Dusp9*+/- ESCs, and *Zic3*+/- ESCs) and iPSCs (male iPSC lines 4, 8, 16; female iPSC lines 20, 21, 22; both early and late passages) grown in S/L condition were differentiated in the absence of feeders by LIF withdrawal (similar as mouse ESC medium but with 10% FBS and without LIF) at a cell density of $4*10^4$ cells/cm^2 for two days, during which medium was refreshed daily and cells were harvested at different time points (0h, 24h and 48h), as previously described (Schulz et al., 2014). Likewise, male iPSC lines overexpressing X-linked genes were differentiated by LIF withdrawal with 5 µg/mL blasticidin in the absence of feeders.

Clonal assays

iPSCs were subjected to LIF withdrawal, and 5000 cells were sorted onto feeders in S/L in each well of a 12-well plate in triplicate at 0h, 24h, 48h, 72h of LIF withdrawal. The next day cultures were switched to 2i/L. Alkaline Phosphatase (AP) staining was carried out 5 days after replating, using the VECTOR Red Alkaline Phosphatase (Red AP) Substrate Kit (VECTOR, SK-5100). Imaging was carried out using an Nikon Eclipse Ti2 Microscope equipped with an Nikon DS-Qi2 camera. AP positive colonies in each well of the 12-well plates were counted using NIS Element Auto Measurement.

Cell growth assay

ESCs and iPSCs were plated in 24-well plates at a cell density of $4*10^4$ cells/cm^2 for two days, during which medium was refreshed daily and cells were counted at different time points (0h, 12h, 24h, 36h and 48h). The cell numbers are presented as fold changes relative to cell numbers at 0h.

FUCCI cell-cycle reporter assay

We generated XY and XX Mus/Cas ESCs expressing the FUCCI fluorescent reporters together with an H2B nuclear marker by co-transfecting of the WT XY and XX ESCs with PB expression constructs including PB-mCherry-hCdt1-BSD, PB-mVenus-hGeminin-PURO and PB-mCerulean-H2B-NEO (Waisman et al., 2017) and pCAGP Base (Silva et al., 2009) using Lipofectamine 2000. Transfected cells were selected with 20 µg/mL blasticidin, 2 µg/mL puromycin and 100 µg/mL G418 supplemented to the medium for two days starting from 24h after transfection and maintained with 5 µg/mL blasticidin, 1 µg/mL puromycin and 50 ug/ml G418 thereafter. The BD FACSMelody cell sorter were used to analyze the FUCCI ESCs at different phases of the cell cycle.

EdU incorporation assay

ESCs and iPSCs were pulse-labeled with the Click-iT EdU Alexa Fluor 647 Flow Cytometry Assay Kit (Invitrogen, C10424) according to the manufacturer's instructions. Briefly, cells were incubated with 10µM 5-ethynyl-2′-deoxyuridine (EdU) for 45 min at 37°C. Then, cells were detached from plates with 0.05% Trypsin-EDTA (Gibco, 25300054), washed with PBS/ 2% BSA and aliquoted into one million cells per tube. Cells were fixed with 4% PFA for 20 minutes, washed with PBS/ 2% BSA and followed by 20 minutes permeabilization with PBS/ 0.5% Triton X-100. Cells were further incubated with the staining cocktail for 10 minutes at room temperature in the dark to reveal EdU incorporation. After twice washes with PBS/ 2% BSA, cells were stained with 3µM PI (Invitrogen, P1304MP) for 15 minutes at room temperature and analyzed using the BD FACSCanto II HTS flow cytometer.

Immunofluorescence

Immunofluorescence analyses were carried out largely as described previously (Pasque et al., 2014), using the following primary antibodies: NANOG (eBioscience, 14-5761 clone eBioMLC-51, 1/200; and Abcam, ab80892, 1/ 200), DPPA4 (R&D, AF3730, 1/200), HA (Cell Signaling Technology, 2367S, 1/100), DUSP9 (Abcam, ab167080,

1/100). Images were acquired using an ApoTome Zeiss Microscope equipped with an AxioCam MRc5 camera. ESC and iPSC lines were defined as NANOG+ or DPPA4+ when >50% cells showed NANOG or DPPA4 staining signal.

RNA FISH

RNA Fluorescence In Situ Hybridization (RNA FISH) analyses were carried out mostly as described previously using double stranded directly labelled DNA probe for *Tsix/Xist (Pasque et al., 2014)*. Images were acquired using an ApoTome Zeiss Microscope equipped with an AxioCam MRc5 camera. Single-cell resolution analysis of *Tsix/Xist* biallelic expression in iPSCs and ESCs was determined by calculating the ratio of cells with biallelic *Tsix/Xist* expression to the cells with monoallelic or biallelic *Tsix/Xist* expression.

Genomic DNA extraction and qPCR

Genomic DNA (gDNA) was extracted from feeder-depleted ESCs and iPSCs using the PureLink Genomic DNA Kit (Invitrogen, K1820) and qPCR was performed using the Platinium SYBR Green qPCR SuperMix-UDG kit (Invitrogen, 11733046) on a ABI ViiA7 real-time PCR system (Applied Biosystems), following the manufacturer's protocol. Primers against four X-linked genes (*Tfe3, Bcor, Pdha1, and Mid1*) covering the two distal parts of the mouse X-chromosome are listed in S9 Table (Fig 1 G). The standard curve was derived from serial dilutions of gDNA from XY ESCs (V6.5). All qPCR assays used had an efficiency above 95%. Relative quantities of each gene were measured as arbitrary units from comparison to the standard curve. The ratio of X-chromosome to autosome (X/Autosome Ratio) in DNA level was presented as the average ratio of the X-linked gene quantity (*Tfe3, Bcor, Pdha1* and *Mid1*) to the autosomal gene quantity (*Gapdh*), in other words X/Autosome Ratio = (*Tfe3/Gapdh + Bcor/Gapdh + Pdha1/Gapdh + Mid1/Gapdh*)/4 .

RT-qPCR

Total RNA was extracted using the RNeasy Mini Kit (Qiagen, 74106) or TRIzol (Invitrogen, 15596026). cDNA synthesis was performed using the SuperScript III First-Strand Synthesis SuperMix kit (Invitrogen, 11752-050) and RT-qPCR was performed using the Platinium SYBR Green qPCR SuperMix-UDG kit (Invitrogen, 11733046) and on the ABI ViiA7 real-time PCR system, following the manufacturer's protocol. Primers used are listed in S9 Table. The standard curve was derived from serial dilutions of cDNA. All assays used had an efficiency above 95%. Relative quantities of each transcript were calculated as arbitrary units from comparison to the standard curve. Relative expression level of the target transcript was presented as the ratio of the target transcript quantity to the housekeeping transcript (Gapdh) quantity. Logarithm values (base 2) of relative expression levels were used for assessment of the gene expression kinetics during differentiation. The relative gene expression levels of five pluripotency-associated genes (*Prdm14, Nanog, Tcl1, Rex1* and *Esrrb*) from iPSCs (male lines: 1, 4, 8, 12, 16; female lines: 19, 20, 21, 22, 23, 26) and ESCs (V6.5 male ESCs and F1-2-1 female ESCs) at 0h and 24h of EpiLC differentiation were used for unsupervised clustering comparison, which was performed in R with heatmap.2 function in package "gplots".

RNA sequencing

Total RNA was isolated from two independent female *Dusp9+/-* ESC lines, *Dusp9+/+* XX and XY ESCs in both the undifferentiated state and the differentiated state after 24 hours of LIF withdrawal using TRIzol following the manufacturer's protocol. 4 µg of total RNA was used for construction of stranded poly(A) mRNA-Seq library with the KAPA stranded mRNA Library prep kit (KAPA Biosystems, KK8421). Library concentrations were quantified with the Qubit dsDNA HS (High Sensitivity) Assay Kit (Invitrogen, Q32854), and equimolar amounts were pooled for single-end sequencing on an Illumina HiSeq 4000 instrument (Illumina) to yield ~20 million (range 16-23 million) 36bp or 51bp long reads per sample.

Differential gene expression analysis

Reads from all datasets (*Dusp9+/-* ESCs, *Dusp9+/+* ESCs and XY ESCs) were aligned to mouse reference genome GRCm38/mm10 using STAR (v2.5.3a) with default parameters followed by conversion to BAM format sorted by coordinate. The mapping efficiencies of the datasets were >69% of uniquely mapped reads. Subsequently, the featureCounts function from the R Bioconductor package "Rsubread" was used to assign mapped reads to genomic features. For downstream analyses, only the genes with CPM value (count-per-million) higher than 0.5 in at least two

libraries were retained. The resulting read count matrix (S8 Table) was used as the input for PCA with the top 500 most variable genes. Differential gene expression analysis was performed using the edgeR quasi-likelihood pipeline in R (Chen et al., 2016b). Obtained p-values were corrected for multiple testing with the Benjamini-Hochberg method to control the FDR. DEGs were defined on the basis of both FDR < 0.05 and fold difference ≧ 1.5. Venn diagrams were generated using an online tool as previously described (Heberle et al., 2015). Heatmaps were created using unsupervised hierarchical clustering of both 200 most variable genes (or stem cell maintenance related genes (GO:0019827), MAPK pathway related genes) and the different samples and generated in R using the heatmap.2 function of the package "gplots".

Omni-ATAC-seq

Assay for transposase accessible chromatin (ATAC) followed by sequencing was performed using the Omni-ATAC protocol (Corces et al., 2017). Briefly, iPSCs and ESCs were expanded on top of male WT feeders in mouse ESC medium (S/L condition). After feeder-depletion, 50,000 viable cells were pelleted at 500 RCF at 4°C for 5 min in a fixed angle centrifuge, and then the cells were gently washed once with 50 µl of cold PBS. Next, the cell pellets were resuspended in 50 µl of ATAC-lysis buffer (10mM Tris HCl pH7.4, 10mM NaCl, 3mM MgCl2, 0.1% Tween-20, 0.1% NP40, and 0.01% Digitonin) and incubated on ice for 3 min. Wash out lysis with 1 ml of cold ATAC-lysis buffer containing 0.1% Tween-20 but No NP40 or digitonin and invert tube 3 times to mix. Nuclei were pelleted at 500 RCF for 10 min at 4°C in a fixed angle centrifuge. After discarding all supernatant, nuclei were resuspended in 50 µl of transposition mixture (25 ul 2x TD buffer, 2.5 ul transposase (100 nM final), 16.5 ul PBS, 0.5 ul 1% digitonin, 0.5 ul 10% Tween-20, and 5 ul H2O) (Nextera DNA Sample Preparation Kit, Illumina, FC-121-1030). The reaction was performed at 37°C for 30 minutes in a thermomixer with 1000 RPM mixing. The transposed DNA was purified using a Zymo DNA Clean and Concentrator-5 Kit (D4014). DNA libraries were PCR amplified using NEBNext High-Fidelity 2x PCR Master Mix (Bioke, M0541), and size selected for 200 to 800 bp using homemade Serapure beads (Rohland and Reich, 2012). Library concentrations were quantified with the KAPA Library Quantification Kit (KK4854), and equimolar amounts were pooled for single-end sequencing on an Illumina HiSeq 4000 instrument (Illumina) to yield ~50 million (range 34-90 million) 51bp long reads per sample.

Differential chromatin accessibility analysis

Single-end ATAC-seq raw data were analyzed using the ATAC-seq pipeline from the Kundaje lab (Version 0.3.3) (Lee et al., 2016). Briefly, the raw reads were first trimmed using cutadapt (version 1.9.1) to remove adaptor sequence at the 3′ end. The trimmed reads were aligned to reference genome (mm10) using Bowtie2 (v2.2.6) using the '--local' parameter. Single-end reads that aligned to the genome with mapping quality ≥30 were kept as usable reads (reads aligned to the mitochondrial genome were removed) using SAMtools (v1.2). PCR duplicates were removed using Picard's MarkDuplicates (Picard v1.126). Open chromatin regions (peak regions) were called using MACS2 (v2.1.0) using the '-g 1.87e9 -p 0.01 --nomodel --shift -75 --extsize 150 -B --SPMR --keep-dup all --call-summits' parameter (Zhang et al., 2008). The differential chromatin accessibility analysis and related plots were performed using the DiffBind package with 'DESeq2, log2fold=1, FDR<=0.05' parameter (Stark and Brown, 2011). GO analysis for Biological Process terms was performed using GREAT (v3.0.0) analysis (McLean et al., 2010) with the mm10 reference genome, where each region was assigned to the single nearest gene within 1000 kb maximum distance to the gene's TSS.

Motif Discovery Analysis

Known motif search was performed using program of findMotifsGenome.pl in the HOMER package (v4.9.1) with 'mm10 -size -250,250 -S 15 -len 6,8,10,12,16' parameters (Heinz et al., 2010). Incidences of specific motif was examined by the program of annotate-Peaks.pl in the HOMER package with size parameter ''-size 500''.

Western blots

Cells were detached from plates with 0.25% Trypsin-EDTA (Gibco, 25200056), pelleted before addition of RIPA lysis buffer (Sigma, R0278-50ML) supplemented with 1% (v/v) Protease inhibitor cocktail (Sigma, P8340-1ml) and 1% (v/v) Phosphatase inhibitor Cocktail 3 (Sigma, P0044-1ML), and lysed on ice for 30 min. The lysates were spun for 10 min at 13000 rpm. The protein concentration was determined with BCA protein assay kit (Pierce, 23225). Each sample with 15 µg of total protein was denatured in 1x LDS Sample buffer (Life Technologies, NP0007) with 100

mM DTT for 5 min at 98°C. The cell lysates were loaded onto a 4%–15% mini-Protean TGX gel (Bio-Rad, 456-1083), electrophoresed, and transferred to nitrocellulose membranes (VWR,10600002). Membranes were blocked in PBS 0.1% (v/v) Tween-20 and 5% (g/v) blotting reagent (Bio-Rad, 1706404) and incubated with the following primary antibodies overnight at 4°C: rabbit anti-NANOG (Abcam, ab80892, 1/1000), rabbit anti-DUSP9 (Abcam, ab167080, 1/500), mouse anti-DKC1 (Santa Cruz, sc-365731, 1/250), mouse anti-HA (Cell Signaling Technology (CST), 2367S, 1/1000), sheep anti-ZIC3 (R&D Systems, AF5310, 1/250) and mouse anti-ACTIN (Abcam, ab3280, 1/5000). After extensive PBS 0.1% Tween-20 (PBS-T) washes, membranes were incubated with a secondary HRP-conjugated goat anti-mouse IgG antibody (Bio-Rad, 1706516, 1/5000) or goat anti-rabbit IgG antibody (Bio-Rad, 1706515 1/5000) for 30 minutes at room temperature. After another round of extensive PBS-T washes, protein expression was visualized using the ECL chemiluminescence reagent (Perkin-Elmer, NEL103001EA) and LAS-3000 imaging system (Fuji). Data were analyzed with ImageJ.

Single Cell RNA-seq analysis

Single cell RNA-seq data of XX female and XY male ESCs in S/L and 2i/L from published data set (Chen et al., 2016a) was re-aligned to N-masked mouse reference genome mm10 using hisat 2 (2.0.5) with disabled soft-clipping. Alignment was followed by conversion to BAM files using SAMtools 1.4.1, aligned reads were then summarized using featureCounts v1.5.2. Quality controls and downstream analyses were performed with the use of scater and SingleCellExperiment packages (Aaron Lun, Davide Risso, 2017; McCarthy et al., 2017). Cells displaying total counts lower than 500,000 reads and less than 9000 genes detected were discarded from the analysis.

SUPPLEMENTAL REFERENCES

Aaron Lun, Davide Risso (2017). SingleCellExperiment: S4 Classes for Single Cell Data. R package version 1.2.0 (Bioconductor).

Branco, M.R., King, M., Perez-Garcia, V., Bogutz, A.B., Caley, M., Fineberg, E., Lefebvre, L., Cook, S.J., Dean, W., Hemberger, M., et al. (2016). Maternal DNA Methylation Regulates Early Trophoblast Development. Dev. Cell *36*, 152–163.

Carey, B.W., Markoulaki, S., Beard, C., Hanna, J., and Jaenisch, R. (2010). Single-gene transgenic mouse strains for reprogramming adult somatic cells. Nat. Methods *7*, 56–59.

Chen, G., Schell, J.P., Benitez, J.A., Petropoulos, S., Yilmaz, M., Reinius, B., Alekseenko, Z., Shi, L., Hedlund, E., Lanner, F., et al. (2016a). Single-cell analyses of X Chromosome inactivation dynamics and pluripotency during differentiation. Genome Res. *26*, 1342–1354.

Chen, Y., Lun, A.T.L., and Smyth, G.K. (2016b). From reads to genes to pathways: differential expression analysis of RNA-Seq experiments using Rsubread and the edgeR quasi-likelihood pipeline. F1000Res. *5*, 1438.

Chronis, C., Fiziev, P., Papp, B., Butz, S., Bonora, G., Sabri, S., Ernst, J., and Plath, K. (2017). Cooperative Binding of Transcription Factors Orchestrates Reprogramming. Cell *168*, 442–459.e20.

Corces, M.R., Trevino, A.E., Hamilton, E.G., Greenside, P.G., Sinnott-Armstrong, N.A., Vesuna, S., Satpathy, A.T., Rubin, A.J., Montine, K.S., Wu, B., et al. (2017). An improved ATAC-seq protocol reduces background and enables interrogation of frozen tissues. Nat. Methods *14*, 959–962.

Czechanski, A., Byers, C., Greenstein, I., Schrode, N., Donahue, L.R., Hadjantonakis, A.-K., and Reinholdt, L.G. (2014). Derivation and characterization of mouse embryonic stem cells from permissive and nonpermissive strains. Nat. Protoc. *9*, 559–574.

Fulco, C.P., Munschauer, M., Anyoha, R., Munson, G., Grossman, S.R., Perez, E.M., Kane, M., Cleary, B., Lander, E.S., and Engreitz, J.M. (2016). Systematic mapping of functional enhancer-promoter connections with CRISPR interference. Science *354*, 769–773.

Heberle, H., Meirelles, G.V., da Silva, F.R., Telles, G.P., and Minghim, R. (2015). InteractiVenn: a web-based tool for the analysis of sets through Venn diagrams. BMC Bioinformatics *16*, 169.

Heinz, S., Benner, C., Spann, N., Bertolino, E., Lin, Y.C., Laslo, P., Cheng, J.X., Murre, C., Singh, H., and Glass, C.K. (2010). Simple combinations of lineage-determining transcription factors prime cis-regulatory elements required for macrophage and B cell identities. Mol. Cell *38*, 576–589.

Lee, J., Christoforo, G., Christoforo, G., Foo, C.S., Probert, C., Kundaje, A., Boley, N., kohpangwei, Dacre, M., and Kim, D. (2016). kundajelab/atac_dnase_pipelines: 0.3.3.

McCarthy, D.J., Campbell, K.R., Lun, A.T.L., and Wills, Q.F. (2017). Scater: pre-processing, quality control, normalization and visualization of single-cell RNA-seq data in R. Bioinformatics *33*, 1179–1186.

McLean, C.Y., Bristor, D., Hiller, M., Clarke, S.L., Schaar, B.T., Lowe, C.B., Wenger, A.M., and Bejerano, G. (2010). GREAT improves functional interpretation of cis-regulatory regions. Nat. Biotechnol. *28*, 495–501.

Pasque, V., Tchieu, J., Karnik, R., Uyeda, M., Sadhu Dimashkie, A., Case, D., Papp, B., Bonora, G., Patel, S., Ho, R., et al. (2014). X chromosome reactivation dynamics reveal stages of reprogramming to pluripotency. Cell *159*, 1681–1697.

Pasque, V., Karnik, R., Chronis, C., Petrella, P., Langerman, J., Bonora, G., Song, J., Vanheer, L., Sadhu Dimashkie, A., Meissner, A., et al. (2018). X Chromosome Dosage Influences DNA Methylation Dynamics during Reprogramming to Mouse iPSCs. Stem Cell Reports *10*, 1537–1550.

Rohland, N., and Reich, D. (2012). Cost-effective, high-throughput DNA sequencing libraries for multiplexed target capture. Genome Res. *22*, 939–946.

Schulz, E.G., Meisig, J., Nakamura, T., Okamoto, I., Sieber, A., Picard, C., Borensztein, M., Saitou, M., Blüthgen, N., and Heard, E. (2014). The two active X chromosomes in female ESCs block exit from the pluripotent state by modulating the ESC signaling network. Cell Stem Cell *14*, 203–216.

Silva, J., Nichols, J., Theunissen, T.W., Guo, G., van Oosten, A.L., Barrandon, O., Wray, J., Yamanaka, S., Chambers, I., and Smith, A. (2009). Nanog Is the Gateway to the Pluripotent Ground State. Cell *138*, 722–737.

Stark, R., and Brown, G. (2011). DiffBind: differential binding analysis of ChIP-Seq peak data. R Package Version.

Waisman, A., Vazquez Echegaray, C., Solari, C., Cosentino, M.S., Martyn, I., Deglincerti, A., Ozair, M.Z., Ruzo, A., Barañao, L., Miriuka, S., et al. (2017). Inhibition of Cell Division and DNA Replication Impair Mouse-Naïve Pluripotency Exit. J. Mol. Biol. *429*, 2802–2815.

Ying, Q.-L., Nichols, J., Evans, E.P., and Smith, A.G. (2002). Changing potency by spontaneous fusion. Nature *416*, 545–548.

Zhang, Y., Liu, T., Meyer, C.A., Eeckhoute, J., Johnson, D.S., Bernstein, B.E., Nusbaum, C., Myers, R.M., Brown, M., Li, W., et al. (2008). Model-based analysis of ChIP-Seq (MACS). Genome Biol. *9*, R137.